Journal of Materials Chemistry A

Accepted Manuscript

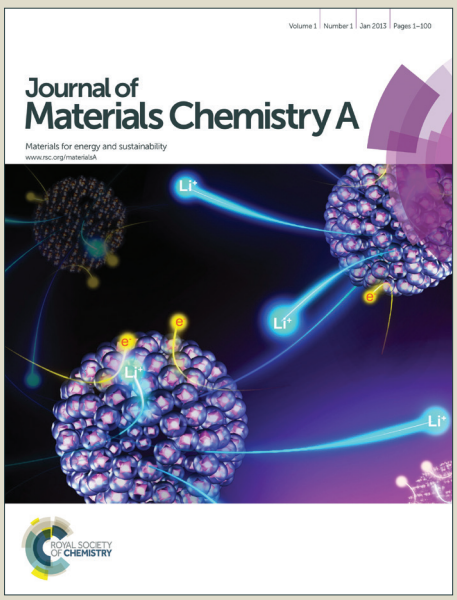

ROYAL SOCIETY OF CHEMISTRY

www.rsc.org/materialsA

Journal of Materials Chemistry

Cite this: DOI: 10.1039/c0jm00000x

www.rsc.org/materials

PAPER

Nanodiamond/carbon nitride hybrid nanoarchitecture as an efficient metal-free catalyst for oxidant- and steam-free dehydrogenation†

Zhongkui Zhao,* and Yitao Dai

Received (in XXX, XXX) Xth XXXXXXXXX 20XX, Accepted Xth XXXXXXXXX 20XX

DOI: 10.1039/c0sc00000x

The nanodiamond/carbon nitride (ND/CNx) nanoarchitectures with the stacked carbon nitride layer covering on nanodiamond have been successfully fabricated through a facile pyrolysis approach of pristine nanodiamond and melamine at the temperature of 650, 700, and 750 ^{o}C, which challenges the long-held axiom that the CNx layer only can be formed at the condensation temperature less than 600 ^{o}C but the it decomposes and inserts into carbon matrix at the temperature higher than 600 ^{o}C. The structure and surface chemical properties of ND/CNx nanomaterials are strongly dependent on pyrolysis temperature and the mass ratio of nanodiamond to melamine. The optimized ND/CNx hybrid carbon nanoarchitecture exhibits synergistically enhanced catalytic performance for direct dehydrogenation of ethylbenzene to styrene under oxidant- and steam-free conditions. The 4.0 mmol g^{-1} h^{-1} of steady-state styrene rate with 99% of selectivity over the developed catalyst can be achieved, but only 2.7 and 2.0 mmol g^{-1} h^{-1} of steady-state styrene rate with 95% and 96% of selectivity can be obtained over the pristine nanodiamond and mesoporous carbon nitride, respectively, under the same reaction conditions, ascribed to the synergistic effect between nanodiamond and carbon nitride of the hybrid material with appropriate CNx layer amount and surface chemical properties. The developed ND/CNx carbon hybrid nanoarchitecture demonstrates 1.48 and 4.15 times the steady-state styrene rate of the established ND and the industrially used K-Fe catalyst, respectively, which allows it to be a potential catalyst for future industrial application for the styrene production through metal-free dehydrogenation of ethylbenzene under oxidant- and steam-free conditions. This work also presents a facile method to create new carbon nitride layer-containing hybrid nanocarbon materials in diverse applications with excellent application properties.

Introduction

Nanodiamonds (ND) powder consists of individual diamond nanoparticles of 5 nm of average diameter were firstly produced in the 1960s in the USSR from soot formed in explosions.[1] In such a preparation process, the detonation of carbon-containing explosives offers both the carbon source and conversion energy, which results in the advantages of being environmental friendly, economic, and suitable for mass production.[1,2] Since the 1990s, ND has become well-known to the world as its possessing excellent mechanical properties for lubrication.[3] Over the past decade, owing to the unique sp^3/sp^2 core-shell structure, highly oxidized surface, large surface-to-volume ratio, high thermal and mechanical stability, exceptional hardness, superior thermal conductivity, wide band gap, optoelectronic properties, as well as biocompatibility, the ND materials have attracted a great deal of attention for their promising applications in the diverse fields including chemical catalysis, photocatalysis, drug delivery, biosensor, field-emission displays, optoelectronic devices, and chromatography separation.[4]

For above, and the many other applications of nanodiamond materials, it's highly desirable for improving their application properties through modifying their structure and the chemical and physical properties.[5] The fabrication of hybrid nanostructures[6] or the introduction of heteroatoms[7] has been considered as a promising approach to adjust the structure and physical and chemical properties of the nanocarbon materials like carbon nanotube, graphene, and mesoporous carbon, but rare papers on the modification of ND were reported. Recently, a graphitic-like carbon nitride material, referred to as g-C_3N_4, has attracted widespread attention because the incorporation of nitrogen atom into carbon matrix can efficiently enhance the catalysis, mechanical, field emission, energy storage, drug delivery, separation, and polluted water purification properties.[8] We also previously demonstrated that the mesoporous carbon nitride materials exhibit much superior catalytic performance in direct dehydrogenation of ethylbenzene to styrene.[9] Furthermore, the carbon nitride-containing carbon nanostructures like graphitic C_3N_4@Carbon and GO/*g*-C_3N_4 have been fabricated and exhibited improved properties for diverse applications including catalysis.[10] Therefore, we envision that the application properties of ND can be hopefully improved by combination of ND and carbon nitride into hybrid nanocomposite through the possible

synergistic effect. However, there are no report on the fabrication of ND/CNx nanocomposite can be found. Generally, the CNx-containing carbon nanosomposites were prepared by immobilizing the CNx on the surfaces of the carbon materials through the in-situ polymerization of carbon nitride precursor at the temperature less than 600 ^{o}C[10a-c,10e,10f] or mixing the as-formed g-C_3N_4 with the other carbon structure.[10a] The former would lead to the surface of carbon nanostructures to be completely covered, but the latter may lead to the maldistribution of CNx on the surface of carbon nanostructures or unformed synergistic effect between CNx and carbon nanostructures. Therefore, the development of a facile and efficient approach for fabricating the CNx-containing carbon hybrid nanocomposites with appropriate amount and distribution of CNx layer on the surface of nanostructures is highly desirable but remains a challenge.

Direct dehydrogenation of ethylbenzene (DDH) to styrene is one of the commercially important reactions in chemical industry. The commercial Fe-K catalyst has some disadvantages like quick deactivation due mainly to potassium loss, unstable Fe^{3+} state, coke-deposition, as well as the caused health injuries to human beings due to the existing chromium in this system. Moreover, the introduction of superheated steam into the feed is indispensable, and it provides the thermodynamic driving force of the reaction as a heat due to its endothermic character, and shifts the chemical equilibrium to higher styrene conversion, besides inhibits the quick deactivation due to coke-deposition.[11] However, it must be noticed that steam is used as large excess molar amount with respect to ethylbenzene (6-13:1); the amount of energy spent is very high (1.5×10^6 kcal per tonne of styrene).[12] The search for new catalyst systems with high stability of Fe^{3+} species and coke-resistance in the absence of potassium or steam is highly required, but a large breakthrough on these issues is in an extremity although many efforts have been made.[13] From the viewpoint of sustainable development, the carbocatalysts are fascinating candidates for DDH of ethylbenzene. However, current efforts are mainly focused on carbon catalyzed oxidative dehydrogenation,[4a,14] and rare report on oxygen- and steam-free direct dehydrogenation can be seen.[4a,9] Therefore, the development of metal-free nanocarbon catalyzed DDH process in the absence of oxidant and steam is highly desirable but remains a rigorous challenge.

ND has emerged as a fascinating candidate for commercially available low-cost but highly-efficient catalyst owing to its unique sp^3/sp^2 core-shell structure, large surface-to-volume ratio, high thermal and mechanical stability, as well as the wide availability. The defect-rich graphene structure has many chemically active sites; and sp^3 core allows nanodiamond to exhibit high thermal conductivity, which is much favourable for transfer of reaction heat. There has been great interest recently in the use of nanodiamond as metal-free catalysts in diverse reactions.[4a,4e,4f,5a,15] Recently, a charming approach on DDH reaction was reported by using nanodiamond as metal-free and much superior catalyst to carbon nanotube, nanographite, activated carbon, and mesoporous carbon,[4a] which exhibits 2.8 times the steady-state activity of the industrially used K-Fe catalyst. The report makes sail the studies on developing carbon-based catalyst for this reaction, and also exhibits a huge potential for industrial application. Graphitic carbon nitride material is an appealing material in which the incorporation of nitrogen atoms into the graphitic-like carbon, can significantly improve the application properties in diverse fields including catalysis.[16] The lone electron pairs of nitrogen atoms can form a delocalized conjugated system with the sp^2-hybridized carbon frameworks to change electronic behaviour and also can produce defect sites on carbon surface resulting in great improvement of the reactivity,[10a,17] as well as the introduction of N can improve the basic properties of carbon materials resulting in promotion in dehydrogenation activity but inhibition in cracking side reaction of ethylbenzene by decreasing the amount of phenolic hydroxyl group.[4a,10b,16a,18] We previously demonstrated that the mesoporous carbon nitride material demonstrated the superior catalytic performance for the direct dehydrogenation of ethylbenzene to styrene under oxidant- and steam-free conditions.[9] Therefore, we envision that the fabricated ND/CNx nanostructures with appropriate amount of CNx layer may exhibit promising catalytic performance for the DDH reaction via electronic coupling at interface of nanodiamond and CNx layer as well as the change in basic properties.[4a,10b,17b-e,18]

In this work, we report a facile approach for first fabricating ND/CNx hybrid nanostructures containing the appropriate amount stacked carbon nitride (CNx) layer covering on ND through pyrolysis of nanodiamond and melamine at the diverse temperature of 650, 700, and 750 ^{o}C, as well as the mass ratio of nanodiamond to melamine (Scheme 1), which challenges the long-held axiom that the CNx only can be formed at the lower pyrolysis temperature less than 600 ^{o}C but the CNx decomposes and inserts into carbon structure while the temperature is higher than 600 ^{o}C.[10a,10c,10d] In a typical synthesis, the desired amount of nanodiamond and melamine was mixed by mechanically milling, and then suffered from a simple pyrolysis process by controllable heating to achieve ND/CNx carbon nanocomposites. The resulting ND/CNx nanostructures were labelled as ND/CNx-*T* (*T*=650, 700, 750, and 800 ^{o}C). The obtained materials have been unambiguously characterized by employing sophisticated techniques such as X-ray diffraction (XRD), high-resolution transmission electron microscopy (HRTEM), Field-emission scanning electron microscopy (FESEM), X-ray photoelectron spectroscopy (XPS), Fourier transform infrared spectroscopy (FT-IR), and UV Raman spectroscopy. We also demonstrate for the first time the catalytic performance for DDH of ethylbenzene to styrene, and ND/CNx-750 shows obviously superior catalytic performance to the pristine ND and mesoporous carbon nitride, ascribed to promoting effect of the formed CNx layer in the nanocomposites. The ND has already emerged as a novel and fascinating material with excellent properties in diverse applications like catalysis, luminescence imaging, sensor,

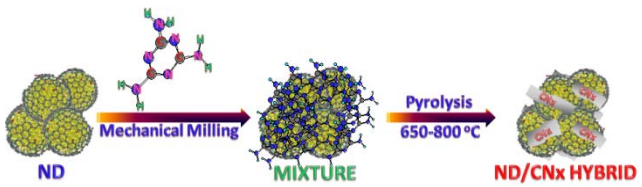

Scheme 1 Schematic illustration for the fabrication of ND/CN*x* nanoarchitectures via a facile pyrolysis approach.

biomolecule separation, drug-delivery, energy conversion and storage, as well as optical and optoelectronic devices,[4,15a-c,19] and therefore we expect that the fabricated ND/CNx nanostructures could be interesting and charming candidates in the above diverse applications. It is also hoped that our findings will simulate exploration and will open a new horizon to form the other carbon nitride layer-containing hybrid carbon nanostructures with new and exciting applications.

Experimental section

Preparation of ND/CN*x* hybrid materials

The commercially supplied nanodiamond synthesized by detonation method followed by acid washing from Beijing Grish Hitech Co. (China) was finely ground with melamine in an agate mortar, and then heated up to desired pyrolysis temperatures in N_2 atmosphere at the certain ramp rate to obtain the final ND/CNx-*T* (*T*=650, 700, 750, and 800 ^oC). Then a series of ND/CNx hybrid nanocomposites with diverse mass ratio of ND to melamine were also prepared by employing similar procedure as above but using 1:5, 1:15, 1:30, and 1:50 of diverse mass ratio of ND to melamine, and the resulting carbon materials are denoted as ND/CNx (1:5), ND/CNx (1:15), ND/CNx (1:30), and ND/CNx (1:50), respectively.

Characterization of ND/CN*x* hybrid materials

X-ray diffraction (XRD) profiles were collected from 10 to 80^o at a step width of 0.02^o using Rigaku Automatic X-ray Diffractometer (D/Max 2400) equipped with a CuKa source (λ = 1.5406 Å). Field emission scanning electron microscope (FESEM) experiments were performed on JEOL JSM-5600LV SEM/EDX instrument. Transmission electron microscopy (TEM) images were obtained by using Tecnai F30 HRTEM instrument (FEI Corp.) at an acceleration voltage of 300 kV. The XPS spectra were carried out on an ESCALAB 250 XPS system with a monochromatized Al Ka X-ray source (15 kV, 150 W, 500 μm, pass energy = 50 eV). FT-IR spectroscopy characterization of catalysts was performed at 150 ^oC under ultrahigh vacuum using a Bruker EQUINOX55 infrared spectrometer. To avoid the fluorescent interference at visible region, the Raman experiments were performed at 244 nm of ultraviolet light region. UV Raman spectra were recorded on a DL-2 Raman spectrometer. A 244 nm line of a LEXEL LASER (95-SHG) was used as the excitation sources. An Acton triple monochromator was used as a spectrometer for Raman scattering. The spectra were collected by a Princeton CCD detector. The power of the laser line at the sample was below 5 mW.

Measurement of catalytic performance

Direct dehydrogenation of ethylbenzene was carried out at 550 ^oC for 20 hours in a stainless steel, fixed bed flow reactor (6 mm O.D.). A catalyst of 25 mg was placed at the centre of the reactor using quartz wool plugs at its two sides. The system was heated to 600 ^oC and kept for 30 min in Ar as the pretreatment of catalyst. After the system was cooled down to 550 ^oC and kept for 10 min, the reactant of 2.8% ethylbenzene with feed flow rate 10 ml min^{-1} and Ar as balance was then fed into the reactor from a saturator kept at 40 ^oC. The effluent from the reactor was condensed in two traps containing ethanol connected in a series. The condensed material was cooled externally in an ice water bath. Quantitative analysis of the collected reaction products (ethylbenzene, styrene, toluene, and benzene) was performed on a FULI 9790 II GC equipped with HP-5 column, 30 m×0.32 mm×0.25 μm, and FID detector. The resulting carbon balance was above 100±4% in all reactions. The styrene rate and selectivity of styrene are used as the evaluation standard for the catalytic performance of the fabricated CNx layer-containing nanocomposites. The styrene rate is the formed styrene molar amount per g catalyst per hour, and the selectivity of styrene is denoted as the percentage of the desired styrene to the total products including the desired styrene and the by-products that containing benzene and toluene.

Results and discussion

The application properties of carbon nanocomposites are notably dependent on the microstructures and surface chemical properties.[4a,20] We expect to obtain ND/CNx nanocomposites with diverse features through varying pyrolysis temperature. FESEM measurements were first performed to characterize the morphology of the fabricated ND/CNx nanostructures and the pristine ND, and the typical FESEM images are presented in Fig. 1. The stacked graphitic carbon nitride layer can be clearly observed for the ND/CNx-650, definitely illustrating the formation of ND/CNx nanocomposite although the sample suffered from pyrolysis at 650 ^oC of high temperature. However, we cannot clearly observe the CNx layer on the other samples, ascribed to the possible decomposition of CNx after it suffered from pyrolysis at higher temperature. In order to establish whether the ND/CNx nanocomposites can be formed at the higher pyrolysis temperature, we further performed the TEM experiments on the fabricated samples and pristine ND. Fig. 2a

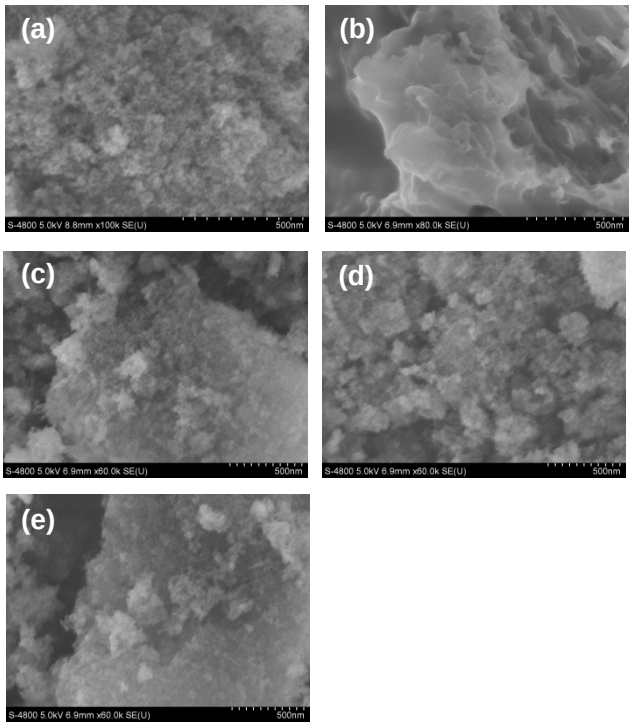

Fig. 1 Typical FESEM images of ND (a) and ND/CNx with diverse pyrolysis temperatures at 650 (b), 700 (c), 750 (d), and 800 ^oC (e).

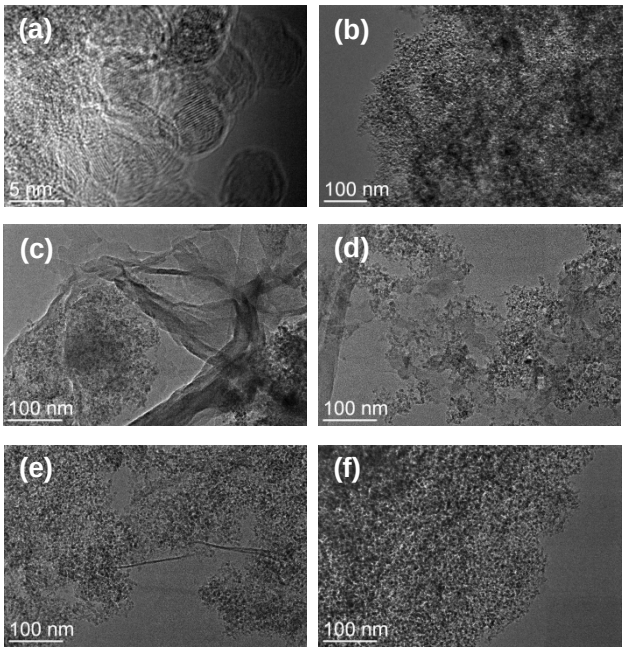

Fig. 2 Typical TEM images of ND (a,b) and ND/CNx with diverse pyrolysis temperatures at 650 (c), 700 (d), 750 (e), and 800 °C (f).

reveals the evidence of the unique core-shell structure of sp^3 C@sp^2 C shell, which is in consistent with the results reported in literatures,[4,9,15d,15e] which allows it to be a bright star in diverse applications with excellent properties. The stacking graphitic carbon nitride layers can be clearly observed for the three samples of ND/CNx-650, ND/CNx-700, and ND/CNx-750 (Fig. 2c, 2d, 2e), which presents a definite evidence that the ND/CNx nanocomposites can be formed even if the pyrolysis temperature reaches up to 750 °C, which challenges the long-held axiom that the CNx only can be formed at the pyrolysis temperature less than 600 °C but the CNx decomposes and inserts into carbon structure to form N-doped carbon materials while the temperature is higher than 600 °C.[10a,10c,10d] However, while the pyrolysis temperature was increased up to 800 °C, the similar morphology (ND/CNx-800, Fig. 2f) to that of pristine ND (Fig. 2b) can be observed, which shows the formed CNx layer appears owing to the decomposition of CNx layer, and therefore N-doped ND but not ND/CNx nanocomposite can be obtained as the too high pyrolysis temperature is used. We tried to obtain CNx by performing the same procedure in the absence of ND, but nothing left, suggesting the ND substrate is essential for CNx formation at a higher temperature. That is to say, the as-prepared materials are the ND/CNx hybrid nanocomposite, but not mechanical mixture, which is further proved by the following XPS analysis and reaction results. The insertion of N atom into ND matrix has been confirmed by the subsequent XPS characterization. Moreover, it can be found that the formation and amount of CNx layer on ND can be adjusted on the basis of the requirement for applications through the change in pyrolysis temperature, which may improve the application properties in many fields or even it has a large potential in extending application fields. The ND/CNx nanocomposite with appropriate amount of CNx layer is beneficial for the DDH of ethylbenzene, but the too thick layer may deteriorate the catalytic performance of ND owing to the surface active sites (C=O) to be covered by CNx layer although the promoting effect of the introduction of CNx in the nanocomposites, confirmed by reaction results and XPS analysis.

The structures of these hybrid materials as well as the parent ND were further investigated by XRD analyses. Besides the characteristic diffraction peaks located at 42.9, 43.9, 75.5, and 91.0 ° corresponding to (100), (111), (022), and (113) diffraction plane of nanodiamond, a peak at 27.2 ° corresponding to the stacked graphitic sheet on all samples can also clearly resolved.[21] On the ND, it comes from the wrapped sp^2 C graphene shell on sp^3 C core, the strengthen peaks around 27.2 ° on the hybrid materials (ND/CNx-650, ND/CNx-700, and ND/CNx-750, especially on ND/CNx-650) can be indexed as (002) peak of the stacking of the conjugated graphitic CNx layers on ND.[10c,10d] Moreover, the similar XRD patterns towards ND/CNx-700, ND/CNx-750, and ND/CNx-800 can be observed, suggesting the similar structure for the samples. In comparison with that of pristine ND, the characteristic diffraction peaks of the composites at 43.9 ° corresponding to (100) and (111) planes become broad and weaker, suggesting the possible de-agglomerating effect of the agglomerated ND. UV Raman was used to further examine the structure of pristine ND and the ND/CNx nanocomposites, besides the nitrogen doping state (Fig. 3b, the UV Raman measurements were adopted to avoid the strong fluorescent interference of CNx-containing samples at visible region). The Raman spectra of ND and ND/CNx-800 exhibits two feature peaks in the range of 1000-2000 cm^{-1} region consisting of well-defined D (1353 cm^{-1}, corresponding to defect and disorder graphene) and G (1600 cm^{-1}, corresponding to pristine graphene), suggesting the existence of exposed graphene nanosheets in the two samples.[22] On the left three samples, we first observe a new peak appearing between D and G peaks, as well as the other new peak around 1275 cm^{-1} is visible on the ND/CNx samples. Correlated to the analysis results, the new peaks can be indexed as the formed CNx layer in the composites, which can be further confirmed by the evidence that the peaks gradually weaken and even disappear with the increase in pyrolysis temperature. The Raman results, correlated to the above FESEM, TEM, and XRD analysis strongly offer a proof that the ND/CNx hybrid nanocomposites with tunable carbon nitride layer have been

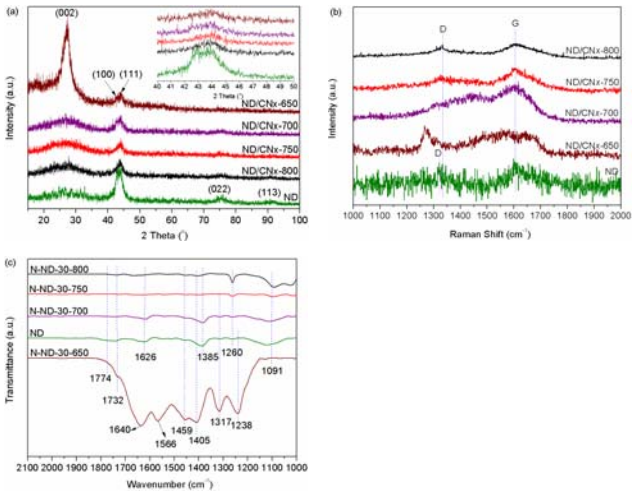

Fig. 3 XRD patterns (a), Raman spectra (b) and FT-IR spectra (c) of ND and ND/CNx nanocomposites with diverse pyrolysis temperatures.

successfully fabricated, and the facile method may be extended to the fabrication of other CNx layer-containing hybrid carbon nanostructures. At the same time, the prepared ND/CNx hybrid nanostructures may extend the applications of ND to broader domains.[4e,4f,5a-c,20d-i] Fig. 3c shows the FT-IR spectra of the samples. The peaks appearing around at 1238, 1317, 1405, 1566, and 1640 cm^{-1} correspond to the typical stretching modes of CN heterocycles.[10a,23] With the increase in pyrolysis temperature, the peaks corresponding to CN structures become weaker, ascribed to the decomposition of graphitic CNx on ND. The peaks at 1091, 1260, 1385, and 1459 cm-1 can be indexed as C-O in C-O-C and C-OH.[4a,10a,23] the peak at 1626 cm^{-1} may be ascribed to the rotational modes of O-H group. The peaks at 1732 and 1774 cm^{-1} correspond to the stretching modes of C=O in carbonyl or carboxy groups.[10a] The carbonyl group has substantial electron density at the oxygen atom, and thus can serves as Lewis base to activate C-H bond in the DDH reaction, however phenolic hydroxyl and carboxyl groups serve as B acidic sites to enhance cracking side reaction of ethylbenzene to form benzene and toluene. The large amount of carbonyl group and the increased electron density is favourable for the desired DDH reaction.

The nature and coordination of the carbon, nitrogen, and oxygen in the fabricated ND/CNx nanocomposites and the pristine nanodiamond were examined by XPS.[17a,24] The XPS survey spectra (Fig. 4a) of the samples shows strong signals from C, N, and O elements, especially the strong peak corresponding to N (38%, Table S2) can be observed on the ND/CNx-650, indicating the ND was wrapped by graphitic carbon nitride layer. The C 1s peak region in the XPS spectra of the samples except for ND/CNx-650 (Fig. 4b and Table S1) was deconvoluted to five peaks at around 284.6, 285.2, 286.0, 287.0, and 288.1-288.3 eV corresponding to C=C , C-N, C-C, C-O (14.7 %), and C=O/C=N, respectively.[22a,22b,24c,25] From Table S1, on the surface of ND/CNx-650, no C-O group, lower C-C (sp^3 core of ND) content, but 26.6% of higher C=C content can be resolved, ascribed to the covering of stacked graphitic CNx layer on the ND, which can be further confirmed by the 53.7% of very high C=N on the composite. Too thick CNx layer on ND of the nanocomposites

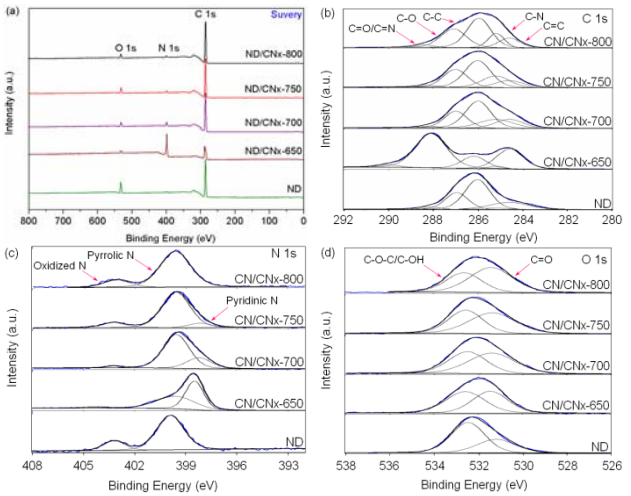

Fig. 4 XPS spectra of pristine ND and the as-prepared ND/CNx nanocomposites with diverse pyrolysis temperatures: (a) Survey spectra; (b) C 1s; (c) N 1s; (d) O 1s.

can cover the surface active sites of catalyst, which deteriorates the catalytic activity of carbon materials. The deconvoluted peak at 290 eV of ND/CNx-650 (2.6%) may be ascribed to the absorbed CO_2 on the CNx layer due to its basicity.[10b,18] The N 1s XPS peak (Figure 4c and Table S2) illustrates that the N atoms in ND/CNx composites (ND/CNx-650, ND/CNx-700 and ND/CNx-750) confirmed by the FESEM, TEM, XRD, and Raman are incorporated into the graphene lattice mainly in a form of "pyridinic N"and "pyrrolic N", and oxidized N, which appear at around 398.2-398.5, 399.6-399.9, and 403.1-430.4 eV, respectively.[22a,22b,24c,25a-c,26] However, on the ND and ND/CNx-800, no Pyridinic N can be resolved, further suggesting the existence of CNx layer on the three samples (ND/CNx-650, ND/CNx-700 and ND/CNx-750). With the increase in pyrolysis temperature from 650 to 800 ^{o}C, the N content decreases from 38% to 2.5%, ascribed to the decomposition of CNx. In all samples, no graphitic N can be observed, which differs from the surface features for the N-doped carbon materials reported in the reference.[4b-d,10a-d,15a-c,17b-e,19] The decreased N content along with the increase in pyrolysis temperature shows the N atom from partially decomposed CNx inserting into hybrid nanocomposite, which is different from the mechanically mixed CNx and nanodiamond. The O 1s XPS spectrum can be deconvoluted into two peaks with the binding energies of 531.2 and 532.8 eV, assigned to C=O and C-O-C/C-OH containing groups (Fig. 4d and Table S3).[4a,14a,27] With the increase in pyrolysis temperature from 650 to 800 ^{o}C, surface O atom content increases from 3.1 up to 5.1 (750 ^{o}C) due to the partially decomposing of CNx layer, and then it decrease to 3.4 at 800 ^{o}C of higher pyrolysis temperature due to the decomposition of surface O-containing groups. Both the total surface O atom content and the C=O group content reach the maximum values (5.4 % and 2.7%, respectively) while the 750 ^{o}C of pyrolysis temperature is employed, allows ND/CNx-750 nanoarchitecture to be an excellent catalyst for DDH reaction since C=O is the catalytically active site.

Herein, we evaluated the catalytic performance of the fabricated ND/CNx composites for the DDH of ethylbenzene to yield styrene under oxidant- and steam-free conditions, and styrene rate and selectivity towards styrene as a function of time on stream are presented in Fig. 5. ND, the established catalyst with superior catalytic performance to diverse carbon structures like carbon nanotube, nanographite, activated carbon, and mesoporous carbon for DDH reaction reported in the literature is included for comparison.[4a] From Fig. 5, the catalytic activity decreases in some degree at the original period, and then keeps at the steady state activity. The initial decrease can be ascribed to the reduction of the highly-active C=O by the formed hydrogen in the reaction process. Furthermore, the results show that the ND/CNx-750 exhibits superior steady-state styrene rate (4.0 mmol g^{-1} h^{-1}) and selectivity (99%) to the other samples. In comparison of the pristine ND, 48% of increased styrene rate on the developed ND/CNx-750 can be obtained (2.7 mmol g^{-1} h^{-1} of styrene rate with 95% of selectivity on the pristine ND). From our previous report,[9] the 2.0 mmol g^{-1} h^{-1} of styrene rate with 96% of selectivity can be obtained over the mesoporous carbon nitride (MCN-1) under the same conditions, even if the developed mesoporous carbon nitride (DUT-1) with the ultrahigh surface area and pore volume was used as dehydrogenation catalyst, the

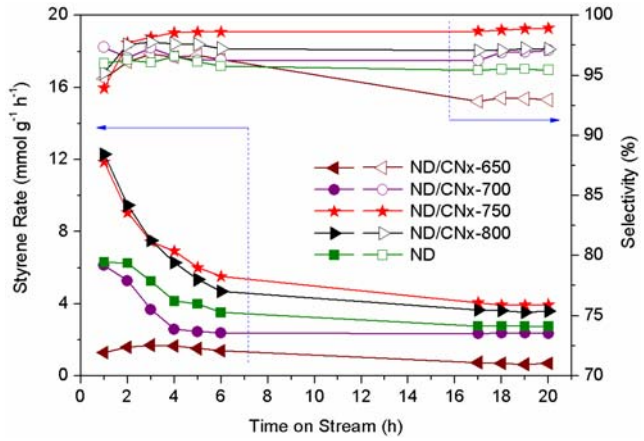

Fig. 5 Catalytic performance of the ND/CNx nanostructures prepared by using diverse pyrolysis temperatures as a function of time on stream for metal-free direct dehydrogenation of ethylbenzene to styrene under oxygen- and steam-free conditions.

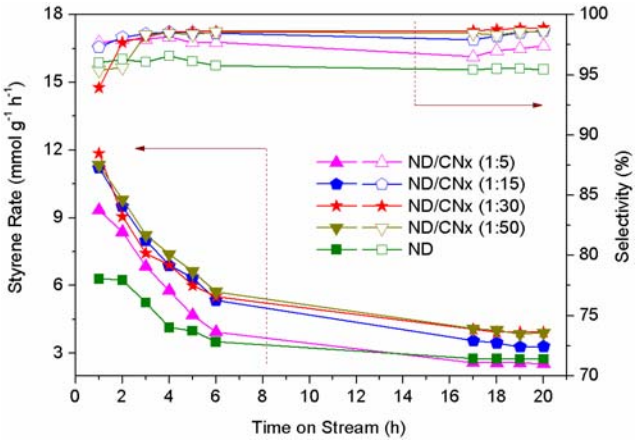

Fig. 6 Catalytic performance of ND/CNx nanostructures prepared with diverse mass ratios of ND to melamine as a function of time on stream for metal-free direct dehydrogenation of ethylbenzene to styrene under oxygen- and steam-free conditions.

only 3.4 mmol g^{-1} h^{-1} of steady-state styrene rate with 94% of selectivity can be achieved. The nonporous CNx material must show the much worse catalytic performance for the DDH reaction. The developed ND/CNx hybrid demonstrates the much superior catalytic performance to the sole ND or CNx, ascribed to the synergistic effect between ND and CNx. Furthermore, we compare the catalytic performance of the developed nanocomposite with the mechanically mixed sample comprising nanodiamond and mesoporous CNx, and the developed hybrid exhibits much better catalytic performance than the mixture, which further demonstrates the formation of hybrid nanoarchitecture but not a mixture. From the XPS, although the surface active C=O decreases owing to the coverage by CNx or to being removed at high pyrolusis temperature, the catalytic performance of the ND/CNx nanocomposite is significantly improved, ascribed to the synergistic effect between ND and CNx. Moreover, the catalytic activity decreases at the initial period and then keeps at a steady-state can be observed. The initial decrease can be ascribed to the reduction of the highly active C=O species on the carbon catalyst surface. Correlating to characterization results from FESEM, TEM, XRD, UV Raman, FT-IR, and XPS shown as above, we can safely say that C=O is the catalytic active sites for DDH reaction, and the microstructure and surface chemical properties of carbon materials is crucial for the DDH reaction. Although the formation of CNx layer in the nanocomposites can improve the electron density of the carbon materials, electron conductivity, and basicity, the too many CNx layer may cover the surface active sites (C=O), and therefore the appropriate CNx coverage is essential for the composite carbon materials to exhibit excellent catalytic performance in the DDH reaction. Furthermore, the pristine ND has 9.4 % of highest surface O-atom content and also 3.1% of highest surface C=O content but worse catalytic performance in DDH reaction than that of ND/CNx-750, which further confirms the promoting effect of the formed CNx layer in the nanocomposite. However, the CNx layer with appropriate amount is crucial for high catalytic performance since the too thick CNx layer may also deteriorates the catalyst by covering the surface active sites.

The mass ratio of ND to melamine may change surface characteristics of ND/CNx nanocomposites, which further affects the catalytic performance, and therefore we further have investigated the optimization of the ND/CNx-750 by varying the mass ratio of ND to melamine from 1:5 to 1:50. Fig. 6 gives the catalytic reaction results. All of the ND/CNx samples show superior styrene rate and selectivity for DDH reaction to pristine ND, suggesting the obviously promoting effect of the introduction of CNx layer in the ND/CNx composites. The styrene rate and selectivity reach maximum value while the mass ratio is 1:30, however the further increase in the relative amount of melamine doesn't lead to the further increase in catalytic performance. The ND/CNx (1:30) may be a promising metal-free catalyst for DDH of ethylbenzene to styrene. In comparison of the established commercially available ND catalyst, the developed ND/CNx demonstrates 1.48 times the steady-state styrene rate of the established ND. On the basis of the comparison results of ND with the industrially used K-Fe catalyst,[4a,9] the developed ND/CNx catalyst has the 4.15 times the steady-state styrene rate of the industrially used K-Fe catalyst, which allows it to be a potential catalyst for future industrial application for the styrene production through metal-free dehydrogenation of ethylbenzene under oxidant- and steam-free conditions.

Then we further characterize the surface features of the samples to reveal the structure-performance relationship of the fabricated ND/CNx nanocomposites in DDH reaction of ethylbenzene by UV Raman (Fig. S1) and XPS (Fig. S3 and Table S4-6) experiments. The UV Raman spectra show that the I_D/I_G (area ratio of D peak to G peak) and the intensity of the peak towards graphitic carbon nitride increase with the enlargement in melamine amount, suggesting the increase in defect-sites and in the amount of carbon nitride layer. From XPS results, the increase in melamine ratio in the parent mixture can increase the surface C=O content ascribed to the protection of CNx to inhibit the decomposition of surface O-containing groups, which enhances the catalytic performance of ND/CNx composite. It further offers an evidence of C=O to be the catalytic active sites for DDH reaction. The ND/CNx nanocomposites have lower C=O content than ND but superior catalytic performance, ascribed to the promotion effect of N from the improved electron density, electronic conductivity and the basicity.[4a,5d,10a,17b-e,28] The

main sideproducts are benzene and toluene resulted from the cracking of ethylbenzene, which consists with the reported results in the literature.[4a] In comparison of the N-doped and undoped carbon materials, the former exhibits significantly superior catalytic performance especially the selectivity. The C=O serving as Lewis bases to activate saturated hydrocarbon for this dehydrogenation reaction has been confirmed,[4a,14a,14c] the surface phenolic hydroxyl group may enhance the cracking of ethylbenzene due to its acidity, since acid sites are active for cracking reaction of hydrocarbon.[18c-e] The introduction of nitrogen atom into carbon matrix can increase the electron density of carbon materials, and therefore strengthens the basicity but weakens the acidity of the catalyst, which may result in an improvement in catalytic activity for styrene production but compressing the benzene and toluene formation. The developed ND/CNx-750 prepared by a facile pyrolysis approach with the 1:30 mass ratio of ND to melamine may be considered as a promising candidate for styrene production through the catalytic DDH reaction of ethylbenzene under oxidant- and steam-free conditions.

Conclusions

In summary, we have demonstrated a facile approach for fabricating nanodiamond/carbon nitride hybrid carbon nanomaterials with diverse CNx layer features, surface structure, surface elemental components and chemical states through pyrolysis of ND and melamine using different pyrolysis temperatures and mass ratio of ND to melamine. The ND/CNx-750 nanocomposite shows much superior catalytic performance, ascribed to the promotion effect of existence of CNx layer with appropriate amount on ND, also to the C=O group- and defect-rich surface feature. The developed catalyst demonstrates 1.48 and 4.15 times the steady-state styrene rate of the established ND catalyst and the industrially used K-Fe catalyst, respectively. The much superior catalytic performance of the ND/CNx to the ND, mesoporous carbon nitride, and even the superhigh surface area mesoporous carbon nitride, suggesting the existence of synergistic effect between ND and CNx layer in the hybrid nanoarchitecture. The unique nanostructure and surface chemical properties of the carbon nanocomposites allow them to be used in diverse fields like catalysis, luminescence imaging, sensor, biomolecule separation, drug-delivery, energy conversion and storage, as well as optical and optoelectronic devices with improved application properties. It's also expected that the facile approach in this work may open a new horizon to fabricate the other novel CNx layer-containing carbon nanoarchitectures for diverse applications.

Acknowledgments

This work is financially supported by the National Natural Science Foundation of China (grant no. 20803006, 21276041, and U1261104), also sponsored by the Chinese Ministry of Education via the Program for New Century Excellent Talents in University (Grant NCET-12-0079).

Notes and references

State Key Laboratory of Fine Chemicals, Department of Catalysis Chemistry and Engineering, School of Chemical Engineering, Dalian University of Technology, Dalian 116024, P.R. China. E-mail: zkzhao@dlut.edu.cn; Fax:+86-411-84986354

† Electronic Supplementary Information (ESI) available: additional Raman spectra, XPS spectra, and all of the quanatitative analysis results from XPS emasurement. See DOI: 10.1039/c0jm00000x/

1 V. Danilenko, *Phys. Solid State.,* 2004, **46**, 595-599.

2 (a) A. Krueger, Adv. Mater., 2008, 20, 2445-2449; (b) Q. Xu and X. Zhao, *J. Mater. Chem.*, 2012, **22**, 16416-16421.

3 N. R. Greiner, D. S. Phillips, J. D. Johnson and F. Volk, *Nature*, 1988, **333**, 440-442.

4 (a) J. Zhang, D. S. Su, R. Blume, R. Schlögl, R. Wang, X. Yang and A. Gajović, *Angew. Chem. Int. Ed.,* 2010, **49**, 8640-8644; (b) H. Huang, E. Pierstorff, E. Osawa, and D. Ho, *Nano Lett.*, 2007, **7**, 3305-3314; (c) M. Ohtani, P. V. Kamat and S. Fukuzumi, *J. Mater. Chem.*, 2010, **20**, 582-587; (d) L. Marcon, F. Riquet, D. Vicogne, S. Szunerits, J. F. Bodart and R. Boukherroub, *J. Mater. Chem*., 2010, **20**, 8064-8069; (e) D. M. Jang, Y. Myung, H. S. Im, Y. S. Seo, Y. J. Cho, C. W. Lee, J. Park, A. Y. Jee and M. Lee, *Chem. Commun.*, 2012, **48**, 696-698; (f) A. Krueger, *J. Mater. Chem.*, 2011, **21**, 12571-12578; (g) X. Q. Zhang, R. Lam, X. Xu, E. K. Chow, H.-J. Kim and D. Ho, *Adv. Mater.*, 2011, **23**, 4770–4775; (h) J. R. Maze, P. L. Stanwix, J. S. Hodges, S. Hong, J. M. Taylor, P. Cappellaro, L. Jiang, M. V. G. Dutt, E. Togan, A. S. Zibrov, A. Yacoby, R. L. Walsworth and M. D. Lukin, *Nature*, 2008, **455**, 644–647; (i) W. Yang, O. Auciello, J. E. Butler, W. Cai, J. A. Carlisle, J. E. Gerbi, D. M. Gruen, T. Knickerbocker, T. L. Lasseter, J. N. Russell, L. M. Smith and R. J. Hamers, *Nat. Mater.*, 2002, **1**, 253-257; (j) Y. R. Chen, H. Y. Lee, K. Chen, C. C. Chang, D. S. Tsai, C. C. Fu, T. S. Lim, Y. K. Tzeng, C. Y. Fang, C. C. Han, H. C. Chang and W. Fann, *Nature Nanotech.,* 2008, **3**, 284-288; (k) V. N. Mochalin and Y. Gogotsi, *J. Am. Chem. Soc.,* 2009, **131**, 4594-4595; (l) A. Krueger and D. Lang, *Adv. Funct. Mater.,* 2012, **22**, 890-906; (m) K. B. Holt, C. Ziegler, D. J. Caruana, J. Zang, E. J. Millán-Barrios, J. Hu and J. S. Foord, *Phys. Chem. Chem. Phys.*, 2008, **10**, 303-310; (n) J. Scholz, A. J. McQuillan and K. B. Holt, *Chem. Commun.*, 2011, **47**, 12140-12142.

5 (a) W. W. Zheng, Y. H. Hsieh, Y. C. Chiu, S. J. Cai, C. L. Cheng and C. Chen, *J. Mater. Chem*., 2009, **19**, 8432-8441; (b) N. Shang, P. Papakonstantinou, P. Wang, A. Zakharov, U. Palnitkar, I. N. Lin, M. Chu and A. Stamboulis, *ACS Nano*, 2009, **3**, 1032-1038; (c) Y. Liang, M. Ozawa and A.Krueger, *ACS Nano*, 2009, **3**, 2288-2296; (d) X. Sun, R. Wang and D. S. Su, *Chin. J. Catal.*, 2013, **34**, 508-523; (e) L. Lai and A. S. Barnard, *J. Mater. Chem*., 2012, **22**, 16774-16780; (f) H. A. Girard, T. Petit, S. Perruchas, T. Gacoin, C. Gesset, J. C. Arnaulta and P. Bergonzo, *Phys. Chem. Chem. Phys.,* 2011, **13**, 11517-11523; (g) Y. L. Hsin, H. Y. Chu, Y. R. Jeng, Y. H. Huang, M. H. Wang and C. K. Chang, *J. Mater. Chem*., 2011, **21**, 13213-13222; (h) K. B. Holt, *Phys. Chem. Chem. Phys*., 2010, **12**, 2048-2058; (i) D. M. Jang, H. S. Im, Y. Myung, Y. J. Cho, H. S. Kim, S. H. Back, J. Park, E. H. Cha and M. Lee, *Phys. Chem. Chem. Phys.,* 2013, **15**, 7155-7160; (j) I. Kratochvílová, A. Kovalenko, F. Fendrych, V. Petráková, S. Zálišd and M. Nesládek, *J. Mater. Chem.*, 2011, **21**, 18248-18255; (k) P. Neumann,I. Jakobi, F. Dolde, C. Burk, R. Reuter, G. Waldherr, J. Honert, T. Wolf, A. Brunner, J. H. Shim, D. Suter, H. Sumiya, J. Isoya and J. Wrachtrup, *Nano Lett.*, 2013, **13**, 2738-2742; (l) R. Lam, M. Chen, E. Pierstorff, H. Huang, E. Osawa and D. Ho, *ACS Nano*, 2008, **2**, 2095-2102; (m) H. Huang, E. Pierstorff, E. Osawa and D. Ho, *ACS Nano,* 2008, **2**, 203-212; (n) A. V. Okotrub, L. G. Bulusheva, V. L. Kuznetsov, D. V. Vyalikh and M. V. Poyguin, *Eur. Phys. J. D*, 2005, **34**, 157-160.

6 (a) J. Yu, G. Liu, A. V. Sumant, V. Goyal and A. A. Balandin, *Nano Lett.*, 2012, **12**, 1603-1608; (b) Y. Wang, M. Jaiswal, M. Lin, S. Saha, B. Ozyilmaz and K. P. Loh, *ACS Nano*, 2012, **6**, 1018-1025; (c) D. Zhang, T. Yan, L. Shi, Z. Peng, X. Wen and J. Zhang, *J. Mater. Chem.* 2012, **22**, 14696-14704; (d) J. H. Lee, N. Park, B. G. Kim, D. S. Jung, K. Im, J. Hur and J. W. Choi, *ACS Nano,* 2013, **7**, 9366-9374; (e) M. Zhao, Q. Zhang, J. Huang and F. Wei, *Adv. Funct. Mater.,* 2012, **22**, 675-694; (f) L. L. Zhang, Z. Xiong and X. S. Zhao, *ACS Nano* 2010, **4**, 7030-7036; (g) L. Lu, J. Liu, Y. Hu, Y. Zhang, H. Randriamahazaka and W. Chen, *Adv. Mater.* 2012, **24**, 4317-4321; (h)

Y. Li, W. Zhou, H. Wang, L. Xie, Y. Liang, F. Wei, J. Idrobo, S. J. Pennycook and H. Dai, *Nat. Nanotechnol*., 2012, **7**, 394-400.

7 (a) N. Yang, H. Uetsuka, E. Osawa and C. E. Nebel, *Nano Lett.*, 2008, **8**, 3572-3576; (b) Y. Gao, G. Hu, J. Zhong, Z. Shi, Y. Zhu, D. Su, J. Wang, X. Bao and D. Ma, *Angew. Chem. Int. Ed.* 2013, **52**, 2109-2113; (c) X. Li, M. Antonietti, *Angew. Chem. Int. Ed.* 2013, **52**, 4572-4576; (d) B. Frank, J. Zhang, R. Blume and R. Schloegl and D. Su, *Angew. Chem. Int. Ed.* 2009, **48**, 6913-6917; (e) F. Gao, G. Zhao, S. Yang, J. J. Spivey, *J. Am. Chem. Soc.*, 2013, **135**, 3315-3318; (f) J. P. Paraknowitsch, A. Thomas, *Energy Environ. Sci.* 2013, **6**, 2839-2855; (g) J. Liang, Y. Jiao, M. Jaroniec, S. Z. Qiao, *Angew. Chem. Int. Ed.*, 2012, **51**, 11496-11500.

8 (a) E. Kroke and M. C. Schwarz, *Chem. Rev.*, 2004, **248**, 493-532; (b) A. Y. Liu and M. L. Cohen, *Science* 1989, **245**, 841-842; (c) Y. Qiu, L. Gao, *Chem. Commun.*, 2003, 2378-2379; (d) P. Dibandjo, L. Bois, F. Chassagneux, D. Cornu, J. M. Letoffe, B. Toury, F. Babonneau and P. Miele, *Adv. Mater.*, 2005, **17**, 571-574; (e) M. Kawaguchi, S. Yagi and H. Enomoto, *Carbon* 2004, **42**, 345-350; (f) J. L. Zimmerman, R. Williams, V. N. Khabashesku and J. L. Margrave, *Nano Lett*., 2001, **1**, 731-734; (g) M. Kim, S. Hwang and J. S. Yu, *J. Mater. Chem.*, 2007, **17**, 1656-1659; (h) Y. J. Bai, B. Lu, Z. G. Liu, L. Li, D. L. Cui, X. G. Xu and Q. L. Wang, *J. Cryst. Growth* 2003, **247**, 505-508; (i) Q. Guo, Q. Yang, L. Zhu, C. Yi, S. Zhang, Y. Xie, *Solid State Commun*., 2004, **132**, 369-374.

9 Z. K. Zhao, Y. T. Dai, J. H. Lin, G. R. Wang. *Chem. Mater.* 2014, **26**, 3151-3161.

10 (a) G. Liao, S. Chen, X. Quan, H. Yu and H. Zhao, *J. Mater. Chem.*, 2012, **22**, 2721-2726; (b) X. H. Li, J. S. Chen, X. Wang, J. Sun and M. Antonietti, *J. Am. Chem. Soc*., 2011, **133**, 8074-8077; (c) Y. Sun, C. Li, Y. Xu, H. Bai, Z. Yao and G. Shi, *Chem. Commun*., 2010, **46**, 4740-4742; (d) Z. Sheng, L.Shao, J. Chen, W. Bao, F. Wang and X. Xia, *ACS Nano*, 2011, **5**, 4350-4358; (e) Y. Zheng, Y. Jiao, J. Chen, J. Liu, J. Liang, A. Du, W. Zhang, Z. Zhu, S. C. Smith, M. Jaroniec, G. Q. Lu and S. Z. Qiao, *J. Am. Chem. Soc.*, 2011, 133, 20116-20119; (f) A. Du, S. Sanvito, Z. Li, D. Wang, Y. Jiao, T. Liao, Q. Sun, Y. H. Ng, Z. Zhu, R. Amal and S. C. Smith, *J. Am. Chem. Soc*., 2012, **134**, 4393-4397.

11 (a) B. D. Herzog, H. F. Raso, *Ind. Eng. Chem. Prod. Res. Dev.*, 1984, **23**, 187-196; (b) M. Baghalha and O. Ebrahimpour, *Appl. Catal. A: Gen.*, 2007, **326**, 143-151; (c) A. C. Oliveira, J. L. G. Fierro, A. Valentini, P. S. S. Nobre, M. do C. Rangel, *Catal. Today*, 2003, **85**, 49-57; (d) D. E. Stobbe, F. R. Van Buren, A. W. Stobbe-Kreemers, A. J. Van Dillen, J. W. Geus, *J. Chem. Soc., Faraday Trans*, 1991, **87**, 1631-1637.

12 (a) O. Shekhah, W. Ranke, A. Schle, G. Kolios and R. Schlögl, *Angew. Chem. Int. Ed*., 2003, **42**, 5760-5763; (b) F. Cavani and F. Trifiro, *Appl. Catal. A: Gen.*, 1995, **133**, 219-239; (c) W. P. Addiego, C. A. Estrada, D. W. Goodman and M. P. Rosynek, *J. Catal*., 1994, **146**, 407-414.

13 (a) F. Cavani, F. Trifiro and A. Vaccari, *Catal. Today*, 1991, **11**, 173-301; (b) P. Kústrowski, A. Rafalska-Łasocha, D. Majda, D. Tomaszewska and R. Dziembaj, *Solid State Ionics*, 2001, **141-142**, 237-242; (c) X. Ye, N. Ma, W. Hua, Y. Yue, C. Miao, Z. Xie and Z. Gao, *J. Mol. Catal. A: Chem*., 2004, **217**, 103-108; (d) N. Mimura, I. Takahara, M. Saito, Y. Sasaki and K. Murata, *Catal. Lett*., 2002, **78**, 125-128; (e) Y. Ohishi, T. Kawabata, T. Shishido, K. Takaki, Q. Zhang, Y. Wang, K. Nomura and K. Takehira, *Appl. Catal. A: Gen.*, 2005, **288**, 220-231; (f) R. J. Balasamy, A. Khurshid, A. A. S. Al-Ali, L. A. Atanda, K. Sagata, M. Asamoto, H. Yahiro, K. Nomura, T. Sano, K. Takehira and S. S. Al-Khattaf, *Appl. Catal. A: Gen.*, 2010, **390**, 225-231; (g) O. Shekhah, W. Ranke and R. Schlögl, *J. Catal.*, 2004, **225**, 56-68.

14 (a) C. Su and K. P. Loh, *Acc. Chem. Res*, 2013, **46**, 2275-2285; (b) L. F. Wang, J. Zhang, D. S. Su, Y. Y. Ji, X. J. Cao and F. S. Xiao, *Chem. Mater.*, 2007, **19**, 2894-2897; (c) J. Zhang, X. Liu, R. Blume, A. Zhang, R. Schlögl and D. S. Su, *Science*, 2008, **322**, 73-77; (d) N. Xiao, Y. Zhou, Z. Ling, Z. Zhao and J. Qiu, *Carbon,* 2013, **60**, 514-522; (e) L. Liu, Q. F. Deng, B. Agula, X. Zhao, T. Z. Ren and Z. Y. Yuan, *Chem. Commun.*, 2011, **47**, 8334-8336; (f) C. Liang, H. Xie, V. Schwartz, J. Howe, S. Dai and S. H. Overbury, *J. Am. Chem. Soc.*, 2009, **131**, 7735-7741; (g) R. Rao, M. Yang, Q. Ling, C. Li, Q. Zhang, H. Yang and4, A. Zhang, *Catal. Sci. Technol.*, 2014, **4**, 665-671; (h) P. Niebrzydowska, R. Janus, P. Kuśtrowski, S. Jarczewski, A. Wach, A. M. Silvestre-Albero and F. Rodríguez-Reinoso, *Carbon*, 2103, **64**, 252-261.

15 (a) X. Liu, B. Frank, W. Zhang, T. P. Cotter, R. Schlögl and D. S. Su, *Angew. Chem. Int. Ed.*, 2011, **50**, 3318-3322; (b) G. P. Bogatyreva, M. A. Marinich, E. V. Ishchenko, V. L. Gvyazdovskaya, G. A. Bazaliĭ and N. A. Oleĭnik, *Phys. Solid State,* 2004, **46**, 738-741; (c) V. S. Bondar, K. V. Purtov, A. P. Puzyr, A. V. Baron, and I. I. Gitel'zon, *Doklady Biochem. Biophys*., 2008, **418**, 11-13; (d) J. Zhang, D. S. Su, A. Zhang, D. Wang, R. Schlögl and C. Hébert, *Angew. Chem. Int. Ed.*, 2007, **46**, 7319-7323; (e) D. S. Su, N. I. Maksimova, G. Mestl, V. L. Kuznetsov, V. Keller, R. Schlögl and N. Keller, *Carbon*, 2007, **45**, 2145-2151.

16 (a) Y. Wang, X. Wang and M. Antonietti, Angew. Chem. Int. Ed., 2012, **51**, 68-89; (b) X. Wang, K. Maeda, A. Thomas, K. Takanabe, G. Xin, J. M. Carlsson, K. Domen and M. Antonietti, *Nat. Mater.*, 2009, **8**, 76-80; (c) M. Tahir, C. Cao, F. K. Butt, F. Idrees, N. Mahmood, Z. Ali, I. Aslam, M. Tanveer, M. Rizwan and T. Mahmood, *J. Mater. Chem. A*, 2013, **1**, 13949-13955; (d) F. E. Osterloh, *Chem. Soc. Rev.*, 2013, **42**, 2294-2320; (e) Y. Zheng, J. Liu, J. Liang, M. Jaroniec and S. Z. Qiao, *Energy Environ. Sci.*, 2012, **5**, 6717-6731; (f) C. Zhu and S. Dong, *Nanoscale*, 2013, **5**, 1753-1767; (g) X. Wang, S. Blechert, and M. Antonietti, *ACS Catal.*, 2012, **2**, 1596-1606.

17 (a) Y. Zheng, Y. Jiao, L. Ge, M. Jaroniec and S. Z. Qiao, *Angew. Chem. Int. Ed.*, 2013, **52**, 3110-3116; (b) K. Gong, F.Du, Z. Xia, M. Durstock and L. Dai, *Science*, 2009, **323**, 760-764; (c) L. S. Panchakarla, A. Govindaraj, C. N. R. Rao, *ACS Nano*, 2007, **1**, 494-500; (d) Z. Wen, X. Wang, S. Mao, Z. Bo, H. Kim, S. Cui, G. Lu, X. Feng, and J. Chen, *Adv. Mater.*, 2012, **24**, 5610-5616; (e) J. Han, L. Zhang, S. Lee, J. Oh, K. Lee, J. R. Potts, J. Ji, X. Zhao, R. S. Ruoff, S. Park, *ACS Nano*, 2013, **7**, 19-26; (f) Y. Zhao, L. Yang, S. Chen, X. Wang, Y. Ma, Q. Wu, Y. Jiang, W. Qian and Z. Hu, *J. Am. Chem. Soc.*, 2013, **135**, 1201-1204.

18 (a) X. Jin, V. V. Balasubramanian, S. T. Selvan, D. P. Sawant, M. A. Chari, G. Q. Lu and A. Vinu, *Angew. Chem. Int. Ed.*, 2009, **48**, 7884-7887; (b) B. Frank, J. Zhang, R. Blume, R. Schlögl and D. S. Su, *Angew. Chem. Int. Ed.*, 2009, **48**, 6913-6917; (c) R. Gounder and E. Iglesia, *J. Am. Chem. Soc.*, 2009, **131**, 1958-1971; (d) D. P. Serrano, J. Aguado and J. M. Escola, *ACS Catal.*, 2012, **2**, 1924-1941; (e) Y. V. Kissin, *Catal. Rev*., 2001, **43**, 85-146; (f) J. Lu, L. Yang, B. Xu, Q. Wu, D. Zhang, S. Yuan, Y. Zhai, X. Wang, Y. Fan and Z. Hu, *ACS Catal.*, 2014, **4**, 613-621.

19 (a) A. Krueger and D. Lang, *Adv. Funct. Mater*., 2012, **22**, 890-906; (b) J. Yu, G. Liu, A. V. Sumant, V. Goyal and A. A. Balandin, *Nano Lett.*, 2012, **12**, 1603-1608; (c) Y. Shao, J. Liu, Y. Wang and Y. Lin, *J. Mater. Chem.*, 2009, **19**, 46-59; (d) G. Xu, W. Zhang, L. Wei, H. Lu and P. Yang, *Analyst*, 2013, **138**, 1876-1885; (e) C. Y. Ko, J. H. Huang, S. Raina and W. P. Kang, *Analyst*, 2013, **138**, 3201-3208.

20 (a) Q. Li, S. Zhang, L. Dai and L. Li, *J. Am. Chem. Soc.*, 2012, **134**, 18932-18935; (b) A. Thomas, A. Fischer, F. Goettmann, M. Antonietti, J. Müller, R. Schlögl and J. M. Carlsson, *J. Mater. Chem*., 2008, **18**, 4893-4908; (c) F. Tao and M. Salmeron, *Science*, 2011, **331**, 171-174; (d) H. Chang and H. Wu, *Adv. Funct. Mater.*, 2013, **23**, 1984-1990; (e) P. Huang, L. Jing, H. Zhu, and X. Gao, *Acc. Chem. Res.*, 2013, **46**, 43-52; (f) D. K. James and J. M. Tour, *Acc. Chem. Res.*, 2013, **46**, 2307-2318; (g) J. Luo, J. Kim and J. Huang, *Acc. Chem. Res.*, 2013, **46**, 2225-2234; (h) D. Jariwala, V. K. Sangwan, L. J. Lauhon, T. J. Marks and M. C. Hersam, *Chem. Soc. Rev.*, 2013, **42**, 2824-2860; (i) P. Neumann,I. Jakobi, F. Dolde, C. Burk, R. Reuter, G. Waldherr, J. Honert, T. Wolf, A. Brunner, J. H. Shim, D. Suter, H. Sumiya, J. Isoya, and J. Wrachtrup, *Nano Lett.*, 2013, **13**, 2738-2742;

21 (a) S. Tomita, A. Burian, J. C. Dore, D. LeBolloch, M. Fujii and S. Hayashi, *Carbon* 2002, **40**, 1469-1474; (b) O. O. Mykhaylyka,Y. M. Solonin, D. N. Batchelder and R. Brydson, *J. Appl. Phys.* 2005, **97**, 74302-74302; (c) J. Chen, S. Z. Deng, J. Chen, Z. X. Yu and N. S. Xu, *Appl. Phys. Lett.* 1999, **74**, 3651-3653.

22 a) J. Y. Kim, W. H. Lee, J. W. Suk, J. R. Potts, H. Chou, I. N. Kholmanov, R. D. Piner, J. Lee, D. Akinwande and R. S. Ruoff, *Adv. Mater.* 2013, **25**, 2308-2313; b) C. Zhang, L. Fu, N. Liu, M. Liu, Y.

Wang and Z. Liu, *Adv. Mater.* 2011, **23**, 1020-1024; c) B. Guo, Q. Liu, E. Chen, H. Zhu, L. Fang and J. R. Gong, *Nano Lett.* 2010, **10**, 4975-4980; d) P. Wu, Y. Qian, P. Du, H. Zhang and C. Cai, *J. Mater. Chem.* 2012, **22**, 6402-6412.

23 G. H. Jun, S. H. Jin, B. Lee, B. H. Kim, W. S. Chae, S. H. Hong and S. Jeon, *Energy Environ. Sci.* 2013, **6**, 3000-3006.

24 (a) W. Li, Z. Zhang, B. Kong, S. Feng, J. Wang, L. Wang, J. Yang, F. Zhang, P. Wu and D. Zhao, D. *Angew. Chem. Int. Ed.* 2013, **52**, 8151-8155; (b) F. Sun, J. Liu, H. Chen, Z. Zhang, W. Qiao, D. Long and L. Ling, *ACS Catal.* 2013, **3**, 862-870; (c) Z. Lin, G. Waller, Y. Liu, M. Liu and C. P. Wong, *Adv. Energy Mater*. 2012, **2**, 884-888.

25 (a) Y. Li, Y. Zhao, H. Cheng, Y. Hu, G. Shi, L. Dai and L. Qu, *J. Am. Chem. Soc.*, 2012, **134**, 15-18; (b) N. Jung, S. Kwon, D. Lee, D. M. Yoon, Y. M. Park, A. Benayad, J. Y. Choi and J. S. Park, *Adv. Mater*., 2013, **25**, 6854-6858; (c L. Shang, T. Bian, B. Zhang, D. Zhang, L. Z. Wu, C. H. Tung, Y. Yin and T. Zhang, *Angew. Chem. Int. Ed.*, 2014, **53**, 250-254.

26 (a) W. Ding, Z. Wei, S. Chen, X. Qi, T. Yang, J. Hu, D. Wang, L. J. Wan, S. F. Alvi and L. Li, *Angew. Chem. Int. Ed.*, 2013, **52**, 11755-11759; (b) G. Wu, N. H. Mack, W. Gao, S. Ma, R. Zhong, J. Han, J. K. Baldwin and P. Zelenay, *ACS Nano*, 2012, **6**, 9764-9776; (c) X. H. Li, S. Kurasch, U. Kaiser and M. Antonietti, *Angew. Chem. Int. Ed*., 2012, **51**, 9689-9692.

27 (a) C. Su and K. P. Loh, *Acc. Chem. Res*, 2013, **46**, 2275-2285; (b) Y. Hou, Z. Wen, S. Cui, X. Guo, J. Chen, *Adv. Mater.*, 2013, **25**, 6291-6297; (c) T. N. Huan, T. V. Khai, Y. Kang, K. B. Shim, H. Chung, *J. Mater. Chem.*, 2012, **22**, 14756-14762.

28 (a) R. D. Holtz, S. B. de Oliveira, M. A. Fraga and M. do C. Rangel, *Appl. Catal. A: Gen.*, 2008, **350**, 79-85; (b) R. J. Balasamy, B. B. Tope, A. Khurshid, A. A. S. Al-Ali, L. A. Atanda, K. Sagata, M. Asamoto, H. Yahiro, K. Nomura, T. Sano, K. Takehira and S. S. Al-Khattaf, *Appl. Catal. A: Gen.*, 2011, **398**, 113-122.